Electronic Supplementary Material (ESI) for Green Chemistry.

Preparation, Characterization and Application of D-Gluconic Acetal-Based Self-Healing Supramolecular Ionogels for Desulphurization of Fuels

Shipeng Chen [a, *], Jinping Wang [a, b], Li Feng [c], Zebin Song,[c] Xiaoji Wang [d, e], Yubin Ke [d], Lin Hua [a], Yange Fan [a], Zheng Li [a], Yimin Hou [a, *], Baoyu Xue [a, *] and Luke Liu [a, *]

[a] Henan Institute of Chemistry, Henan Academy of Sciences, No. 56 Hongzhuan Road, Zhengzhou 450003, China

[b] School of Chemistry and Chemical Engineering, Henan Normal University, Xin xiang, Henan 453007, China

[c] Jiangsu Sunpower Co., Ltd., No 8 of Xingyuan Road, Huangqiao Industrical Park, Taixing 225400, China

[d] Guangdong-Hong Kong-Macao Joint Laboratory for Neutron Scattering Science and Technology, 1 Zhongziyuan Road, Dalang, Dongguan 523803, China

[e] School of Chemical Engineering and Energy Technology, Dongguan University of Technology, Dongguan 523808, China

[*] Authors to whom correspondence should be addressed.

Synthesis

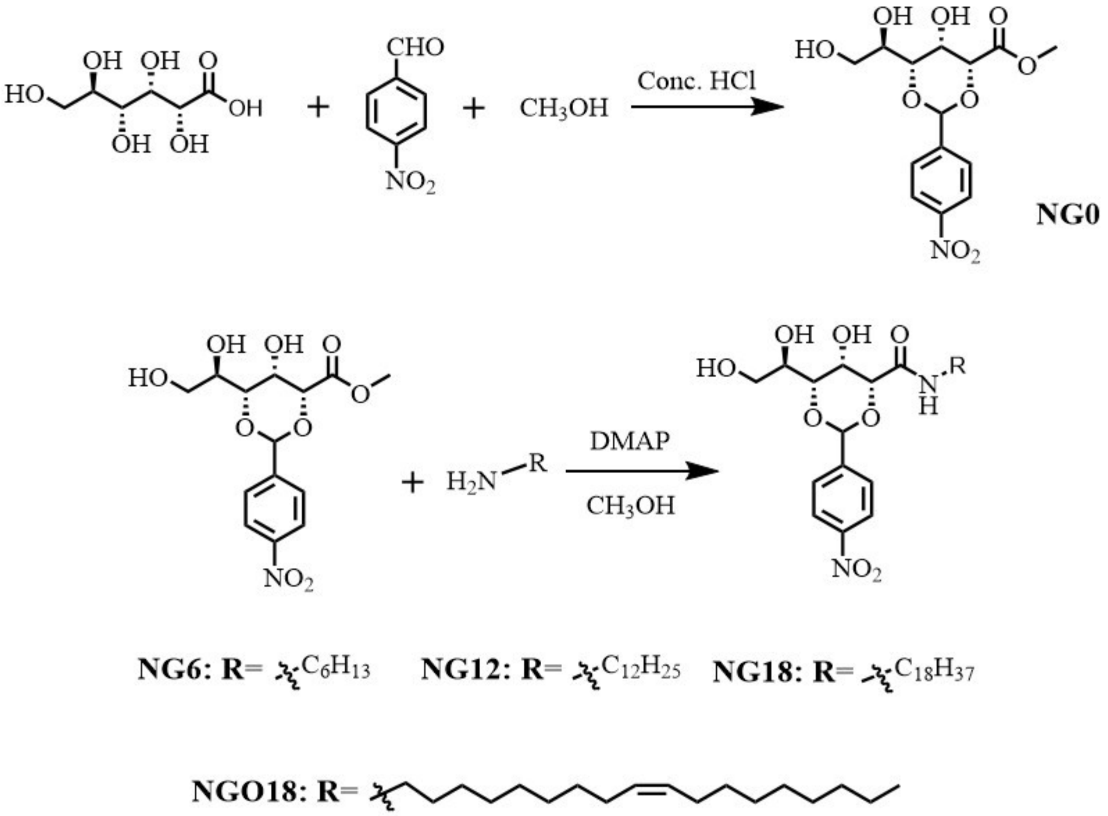

Chart S1. The synthetic routes of NG6, NG12, NG18 and NGO18.

2.1 Synthetic procedures

NG0: 75.56g (0.5 mol) 4-nitrobenzaldehyde was dissolved in 400 ml methanol at room temperature and then 215.8 g 50wt% aqueous solution of D-gluconic acid (0.55 mol) was added to this solution followed by the addition of 200 mL hydrochloride acid (12 mol/L) under vigorously stirring. The reaction mixture was stirred for 5 days and the pale-yellow solid was collected by filtration. The filter cake was recrystallized twice with methanol. Yield: 113.3 g (0.33 mol, 60%).

NG 6, **12**, **18**, and **NGO18**: To a solution of 5.15 g (15 mmol) NG0 in 50 mL methanol was added 42 mmol long chain amine and 0.01 g DMAP (0.008 mmol). The reaction mixture was stirred for 12 h and then 50 ml tert-butyl methyl ether was added. Subsequently，the white solid was collected by filtration. The filter cake was recrystallized with methanol for twice to obtain the product. Yield: 69~83 %.

2.2 Chemical characterization

2, 4− (4−nitro) benzylidene−N− octadecyl −D−gluconamide (NG18)

^{1}H NMR (400 MHz, DMSO-d_6, 25 °C): δ 8.26 (d, 2H), 7.89 (d, 2H), 7.44 (t, J=6.0Hz,1H), 5.80 (s, 1H), 4.74 (t, J=6.0Hz, 2H), 4.48 (s, 1H), 4.41 (s, 1H), 4.03 (d, 1H), 3.81 (d, 1H), 3.67 (s, 1H), 3.58 (d, 1H), 3.45 (m, 1H), 3.11 (m, 2H), 1.42 (s, 2H), 1.23 (s, 30H), 0.86 (t, J=6.4Hz, 3H); The ^{1}H NMR spectrum is shown as the figure below:

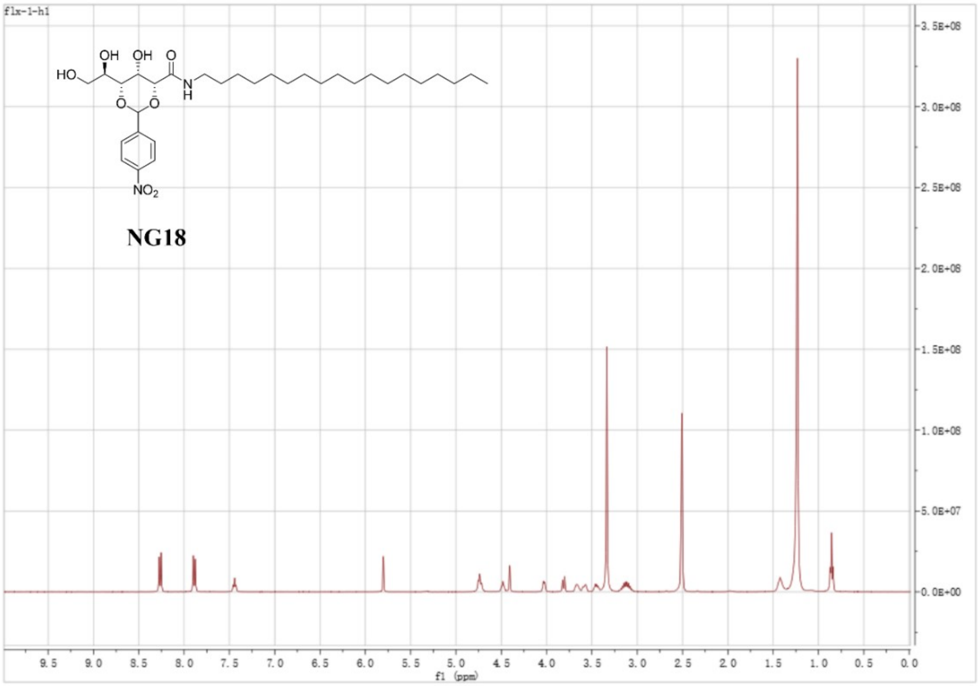

^{13}C NMR (100 MHz, DMSO-d_6, 25 °C): δ 168.2, 148.3, 144.9, 128.4, 123.7, 98.4, 80.7, 79.6, 69.5, 62.9, 62.8, 38.8, 31.8, 29.7, 29.5 (several overlapped signals), 29.3, 29.2, 26.9, 22.6, 14.4. The ^{13}C NMR spectrum is shown as the figure below:

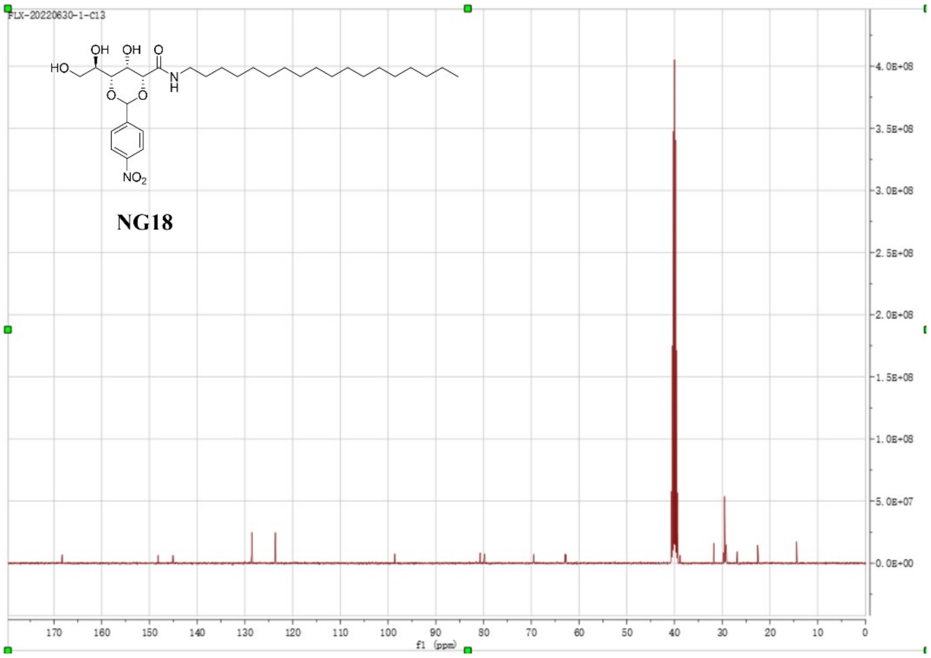

HRMS (ESI): m/z calcd. For $C_{31}H_{52}N_2O_8H^+$ $[M + H]^+$ 581.3796, found 581.3802. The corresponding high resolution mass spectrum is shown as the figure below:

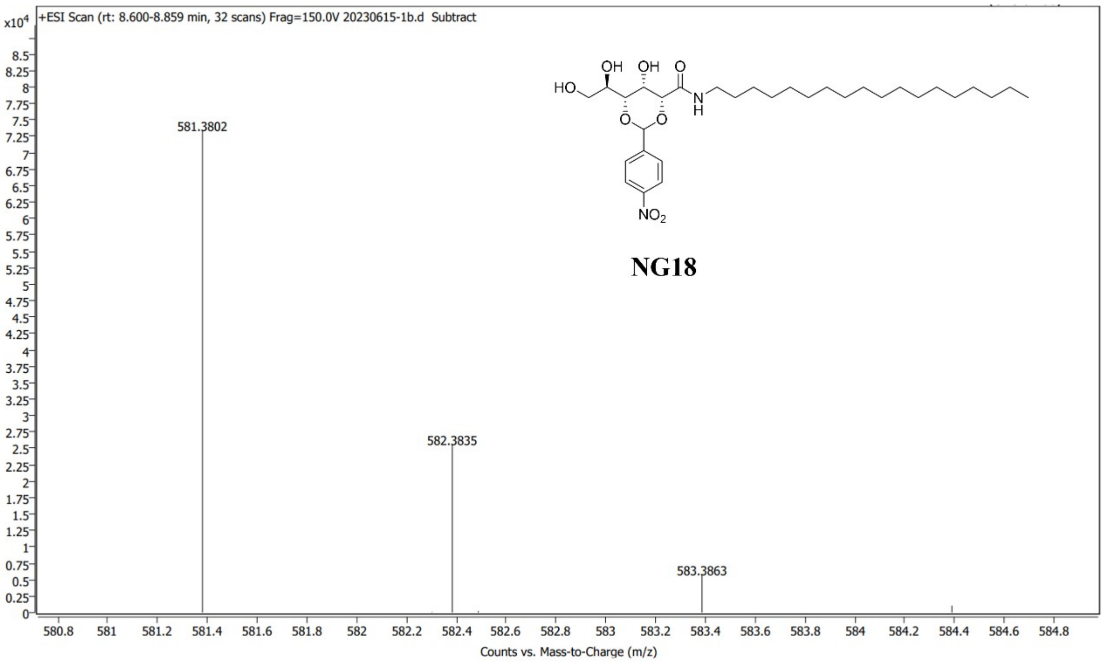

2, 4− (4−nitro) benzylidene−N−Dodecyl−D−gluconamide (NG12)

^1H NMR (400 MHz, DMSO-d_6, 25 °C): δ 8.26 (d, 2H), 7.89 (d, 2H), 7.45 (t, J=6.0Hz, 1H), 5.80 (s, 1H), 4.58(s, 2H), 4.41 (d, 2H), 4.03 (s, 1H), 3.82 (d, 1H), 3.67 (m, 1H), 3.51 (m, 2H), 2.98 (m, 2H), 1.38 (m, 2H), 1.23 (s, 18H), 0.86 (t, J=6.8Hz, 3H); The ^1H NMR spectrum is shown as the figure below:

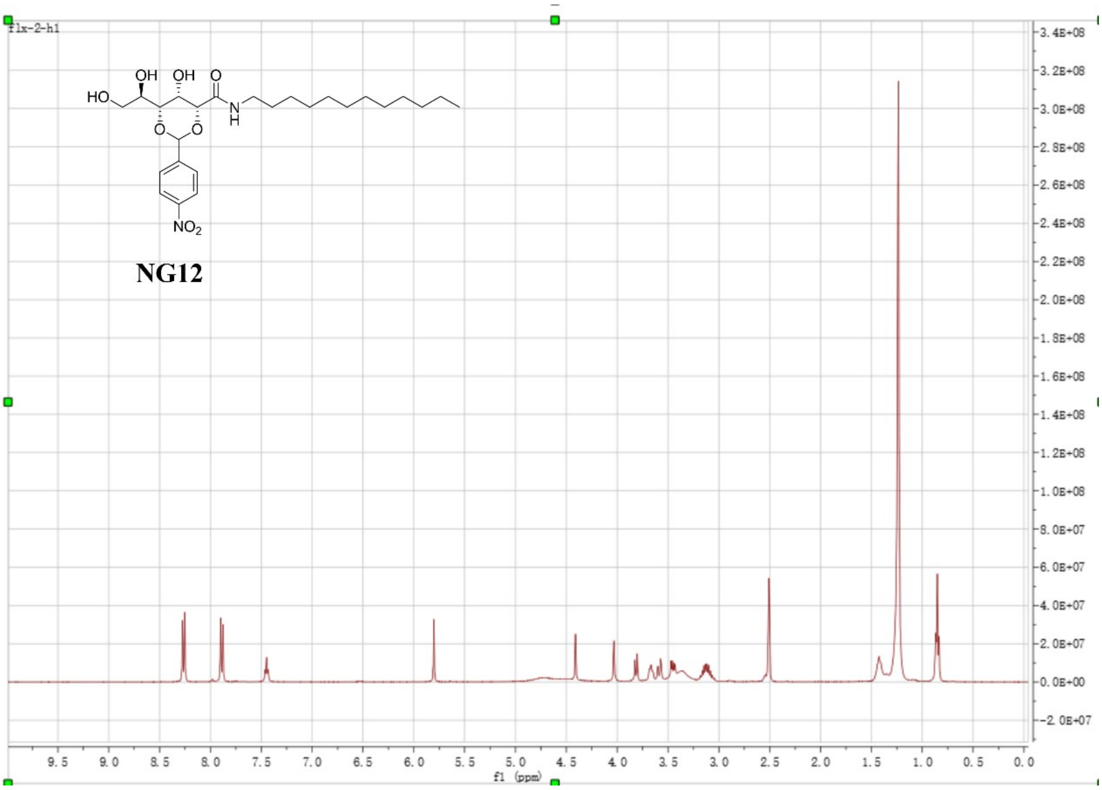

^{13}C NMR (100 MHz, DMSO-d$_6$, 25 °C): δ 168.2, 148.3, 145.1, 128.5, 123.6, 98.6, 80.7, 80.0, 69.4, 62.7, 38.9, 31.8, 29.7, 29.5 (several overlapped signals), 29.3, 29.2, 26.9, 22.6, 14.4. The ^{13}C NMR spectrum is shown as the figure below:

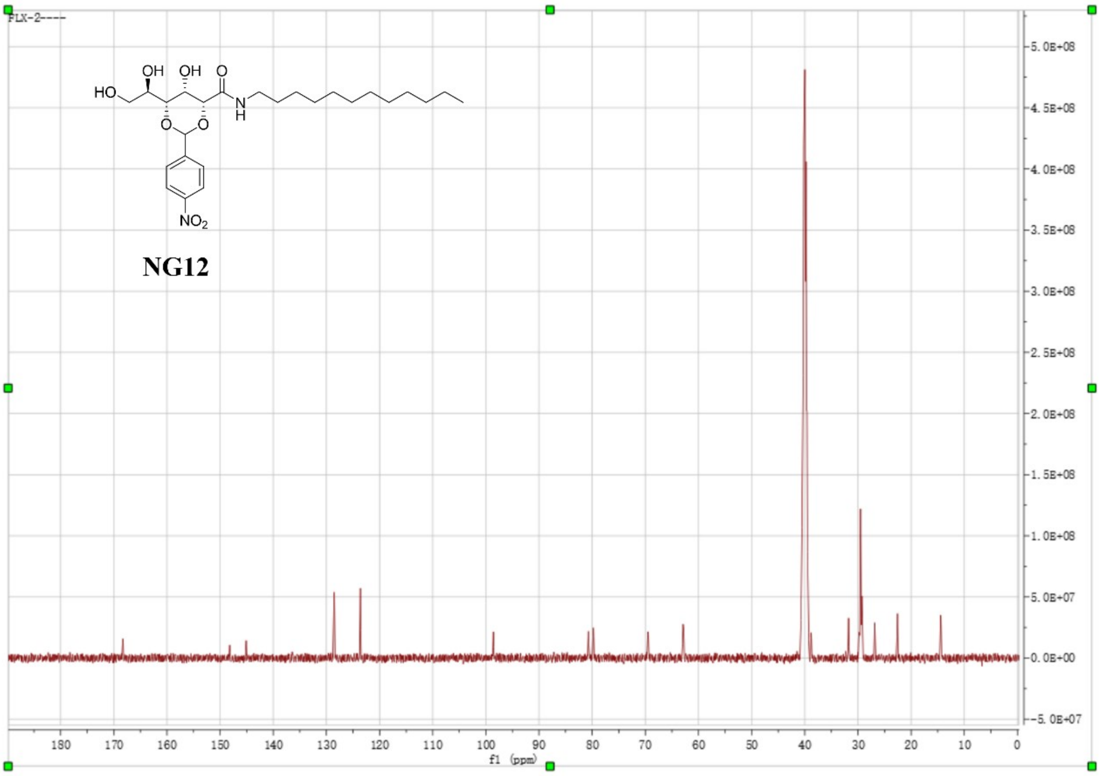

HRMS (ESI): m/z calcd. For $C_{31}H_{52}N_2O_8H^+$ $[M + H]^+$ 497.2857, found 497.2866. The corresponding high resolution mass spectrum is shown as the figure below:

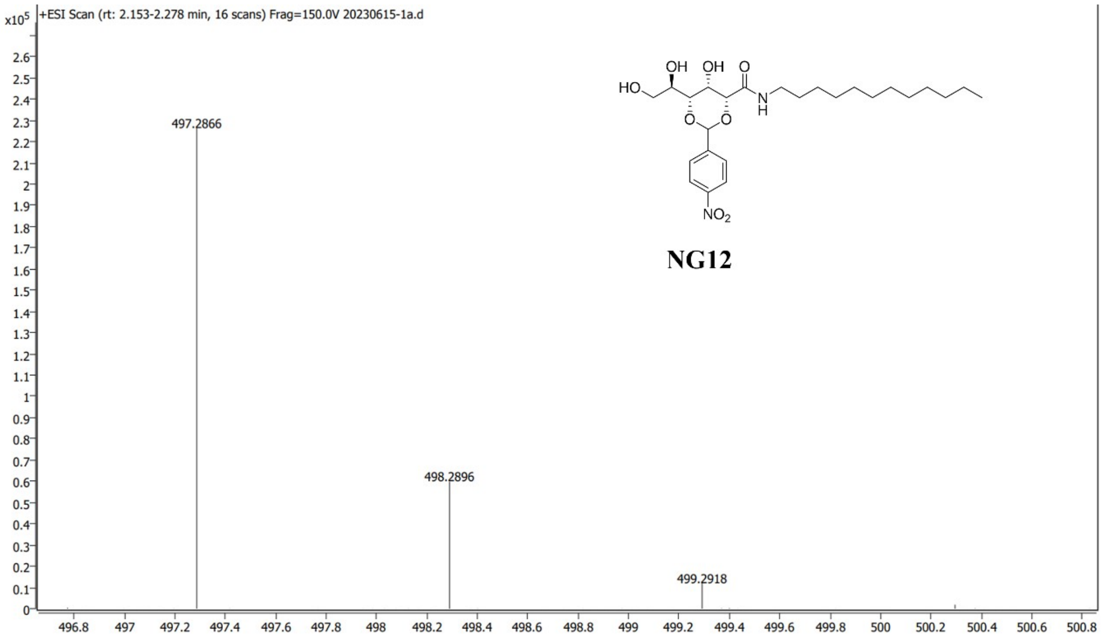

2, 4− (4−nitro) benzylidene−N−Dodecyl−D−gluconamide (NGO18)

^{1}H NMR (400 MHz, DMSO-d_6, 25 °C): δ 8.19 (d, 2H), 7.77 (d, 2H), 7.37 (t, J=6.0 Hz, 1H), 5.73 (s, 1H), 5.27(m, 2H), 4.68 (s, 2H), 4.42 (s, 1H), 4.34 (s, 1H), 3.95 (d, 1H), 3.72 (d, 1H), 3.60 (d, 1H), 3.50 (dd, J_1=11.2 Hz, J_2=2.0 Hz, 1H), 3.37 (m, 1H), 3.05 (m, 2H), 1.90 (m, 4H), 1.34 (dd, J_1=12.4 Hz, J_2=6.4 Hz, 4H), 1.19 (s, 20H), 0.78 (t, J=6.4Hz, 3H); The ^{1}H NMR spectrum is shown as the figure below:

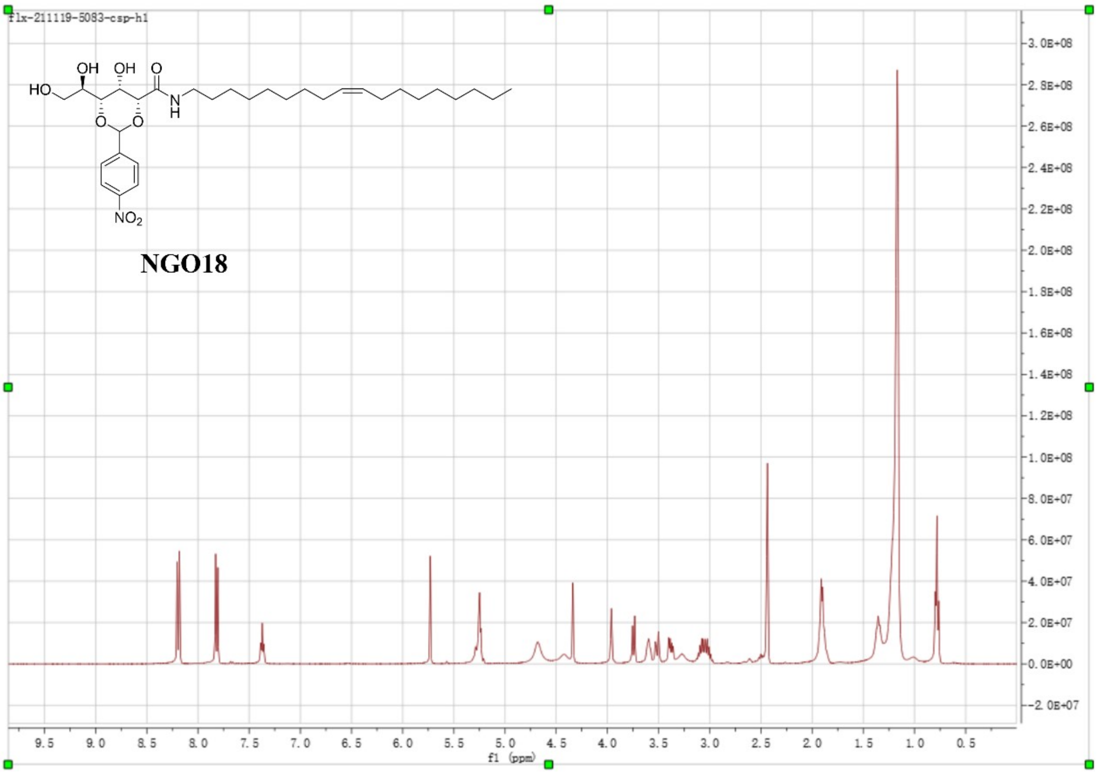

^{13}C NMR (100 MHz, DMSO-d$_6$, 25 °C): δ 168.1, 148.2, 145.2, 130.1, 128.5, 123.6, 98.6, 80.7, 79.8, 69.5, 62.9, 62.8, 38.8, 31.8, 29.7, 29.5 (several overlapped signals), 29.3 (several overlapped signals), 29.1 (several overlapped signals), 27.1, 27.0, 26.9, 22.6, 14.4. The ^{13}C NMR spectrum is shown as the figure below:

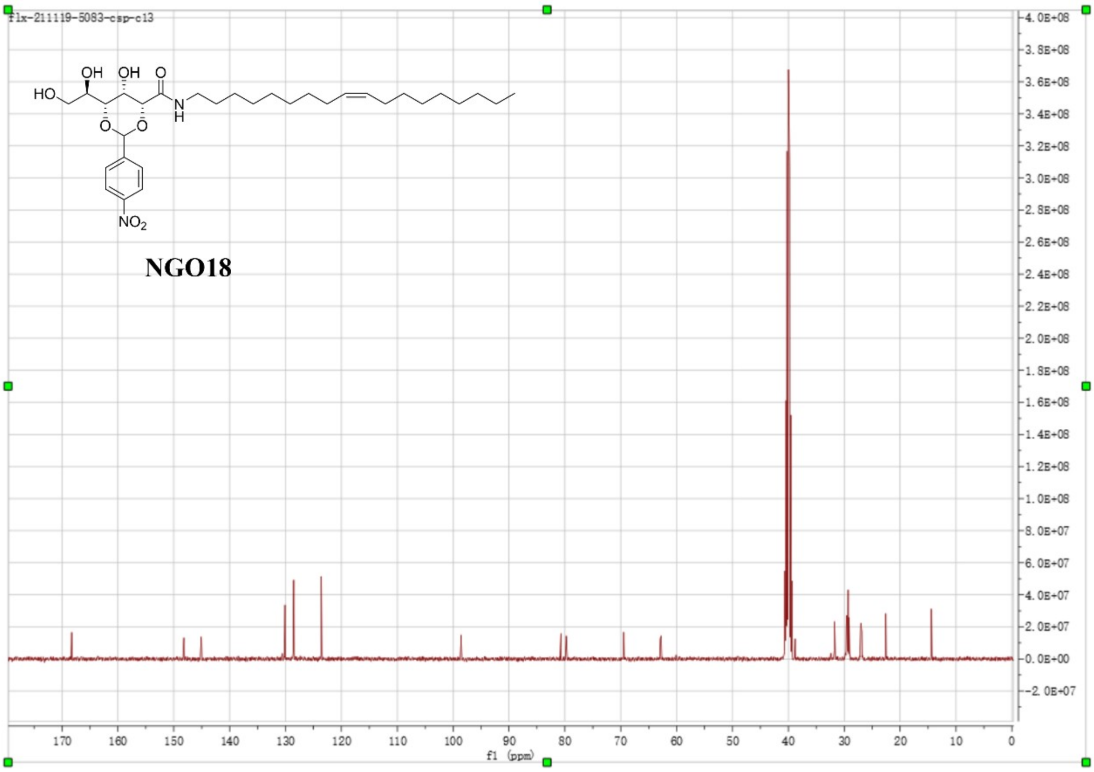

HRMS (ESI): m/z calcd. For $C_{31}H_{52}N_2O_8H^+$ $[M + H]^+$ 579.3640, found 579.3652. The corresponding high resolution mass spectrum is shown as the figure below:

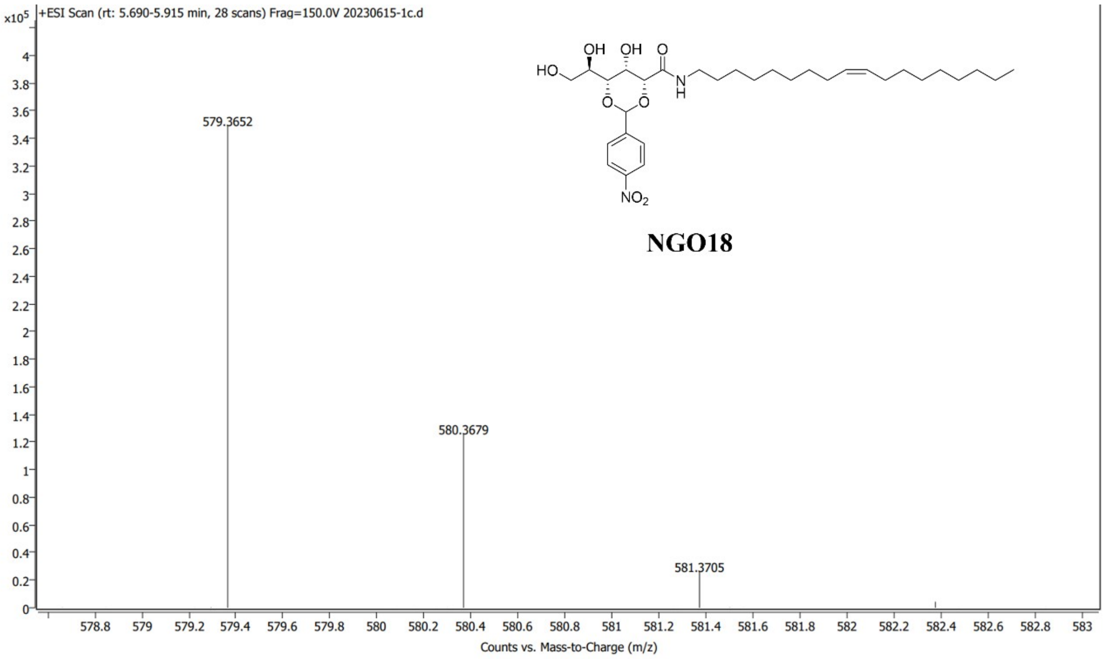

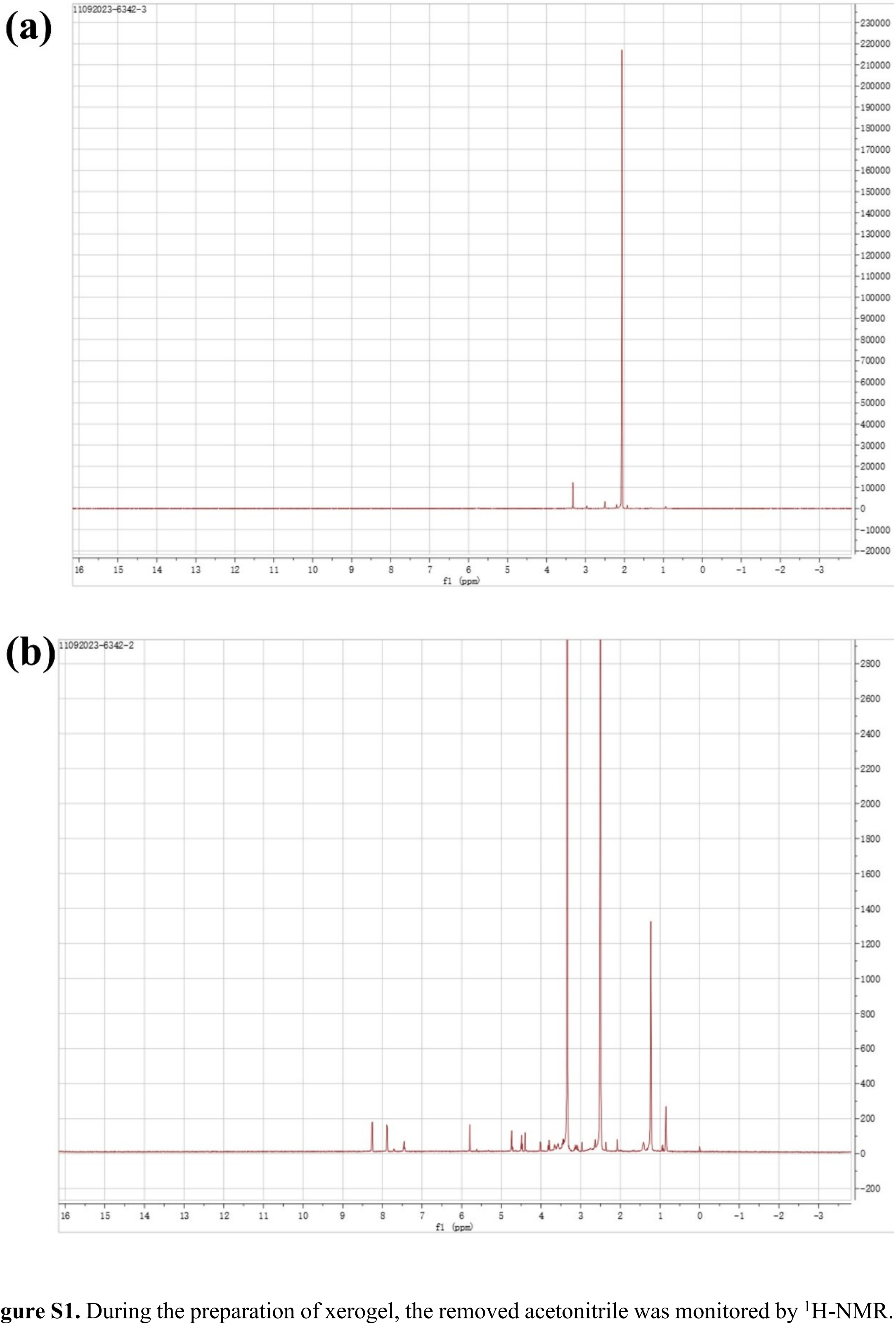

Figure S1. During the preparation of xerogel, the removed acetonitrile was monitored by ^{1}H-NMR. (a) Complete replacement of IL was determined when there was no characteristic peak of IL in the acetonitrile. (b) The prepared xerogel was also investigated by ^{1}H-NMR, no characteristic peak of IL was observed, either.

Figure S2. The SIG loaded with sulphur compounds was dissolved in THF and then stratified after adding water.

Rheological Study

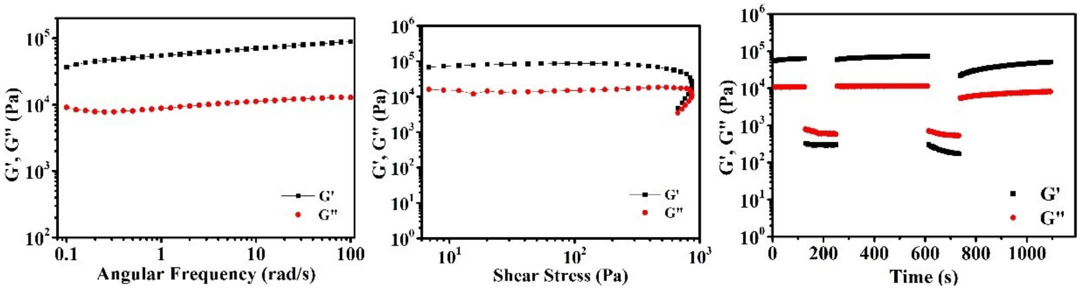

(a) G6-IL2

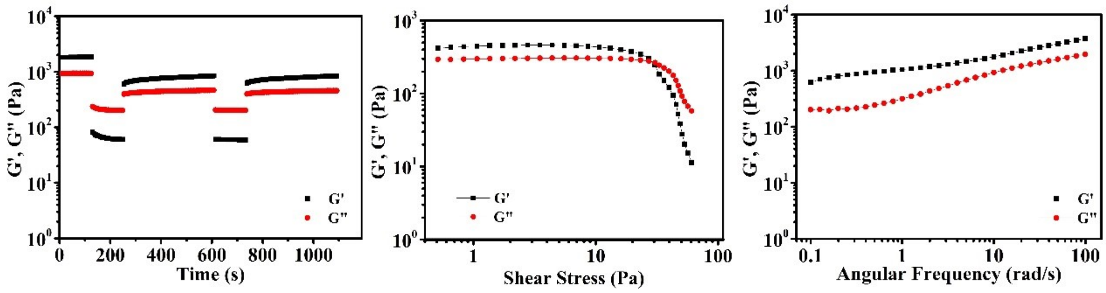

(b) G6-IL3

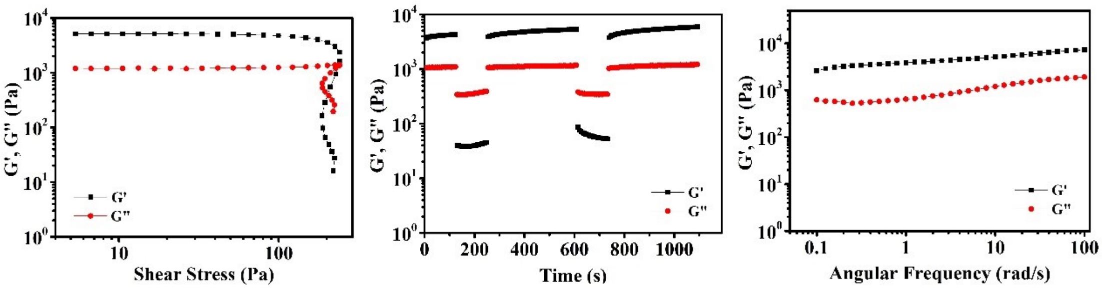

(c) G6-IL4

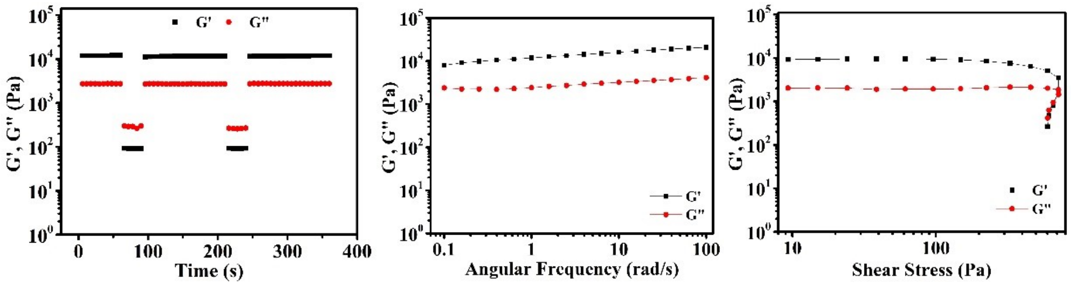

(d) G12-IL2

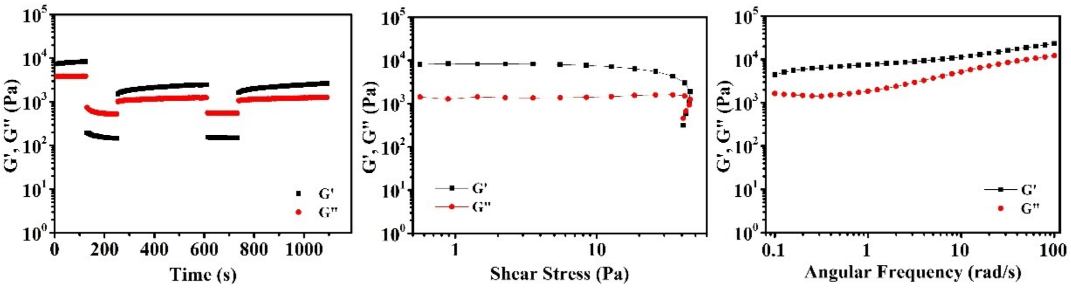

(e) G12-IL3

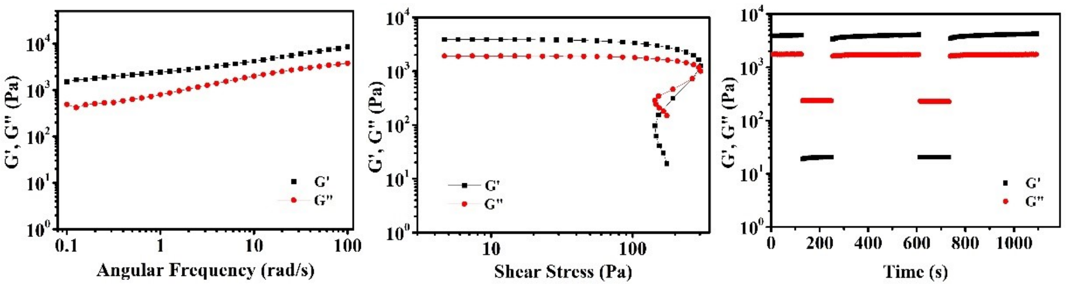

(f) G12-IL4

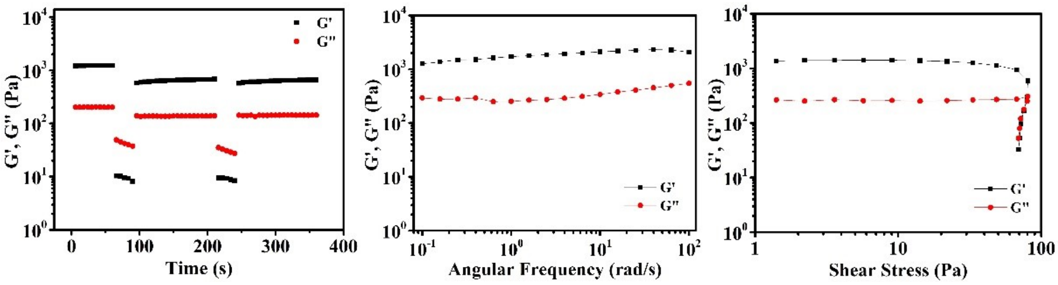

(g) G18-IL1

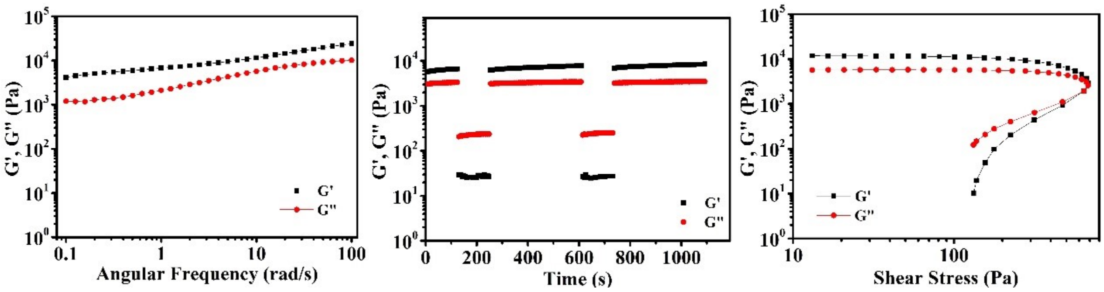

(h) G18-IL2

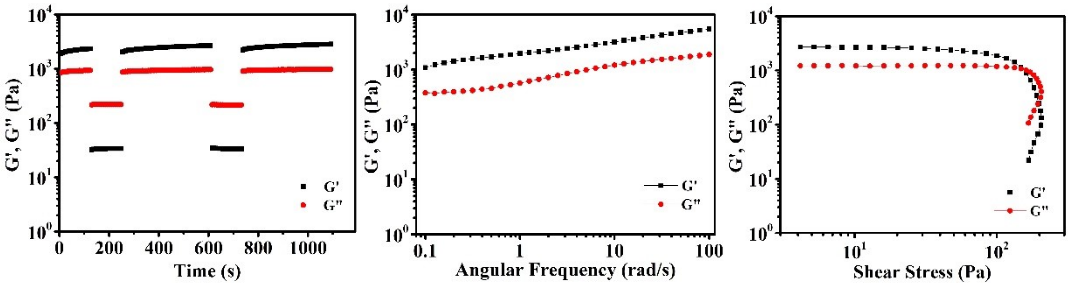

(i) G18-IL3

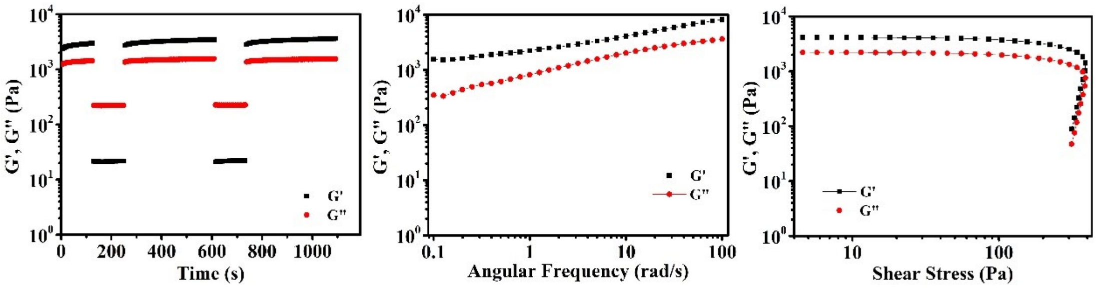

(j) G18-IL4

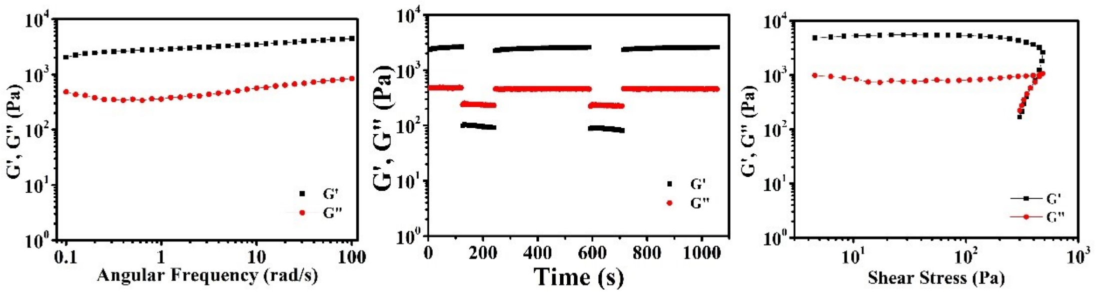

(k) NGO18-IL1

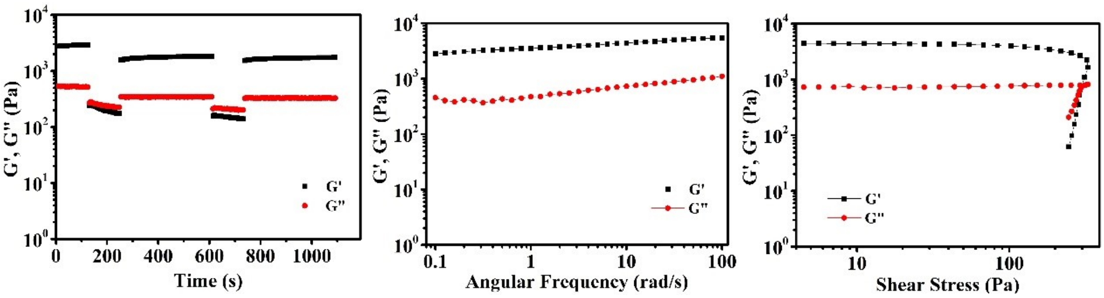

(l) NGO18-IL2

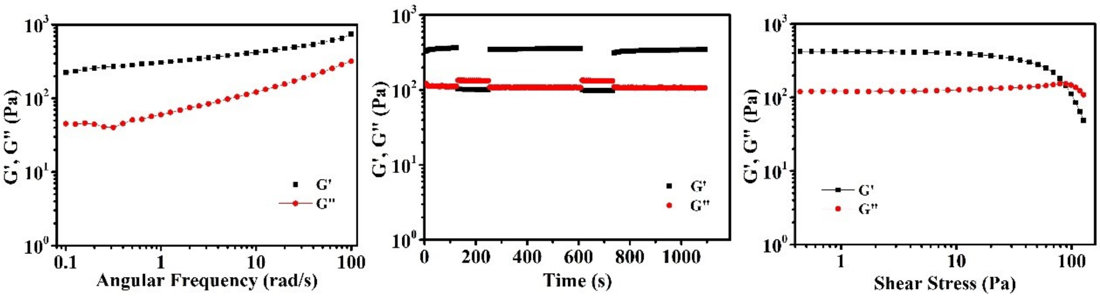

(m) NGO18-IL3

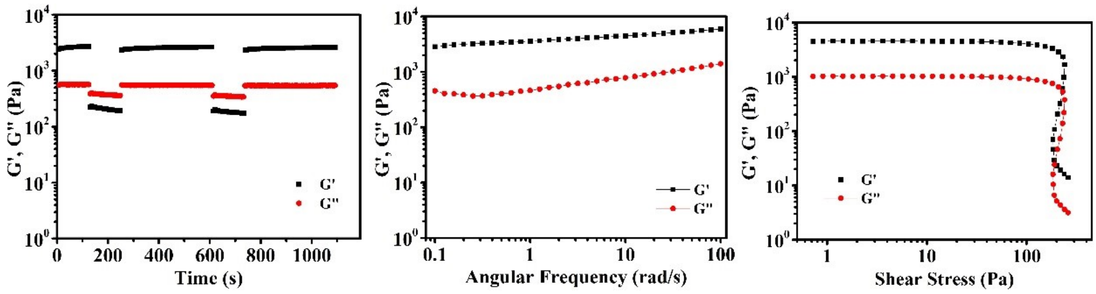

(n) NGO18-IL4

Figure S3. Oscillatory rheological study of SIGs. In each items, from left to right, they are frequency sweep, strain sweep and step-strain measurement, respectively. The detailed rheological data were summarized in **Table S2** below.

Table S1. Rheological data of SIGs (2% w/v) prepared by NG6, NG12, NG18 and NGO18 in 4 ILs

SIGs	G’ (Pa)[a]	G1’ (Pa)[b]	G2’ (Pa)[c]	η (%)	tanδ	Strain stress at flow point (Pa)
NG6-IL2	63943	73811	51201	80.1	0.17	846
NG6-IL3	11847	845	838	7.1	0.51	29
NG6-IL4	4288	5345	5907	100	0.26	244
NG12-IL2	12069	11731	11914	98.7	0.23	715
NG12-IL3	8370	2479	2636	31.5	0.47	45
NG12-IL4	3895	4082	4242	100	0.44	294
NG18-IL1	2631	2591	2597	98.7	0.19	446
NG18-IL2	6647	7754	8435	100	0.52	668
NG18-IL3	2344	2688	2851	100	0.41	157
NG18-IL4	2971	3466	3615	100	0.48	361
NGO18-IL1	1233	678	661	55	0.16	81
NGO18-IL2	2909	1823	1733	60	0.18	289
NGO18-IL3	367	358	345	94	0.31	85
NGO18-IL4	2713	2658	2608	96.1	0.21	240

[a] The initial elastic modulus of the SIGs.

[b] Elastic modulus of the SIGs after the 1st breaking-recovery cycle.

[c] Elastic modulus of the SIGs after the 2nd breaking-recovery cycle.

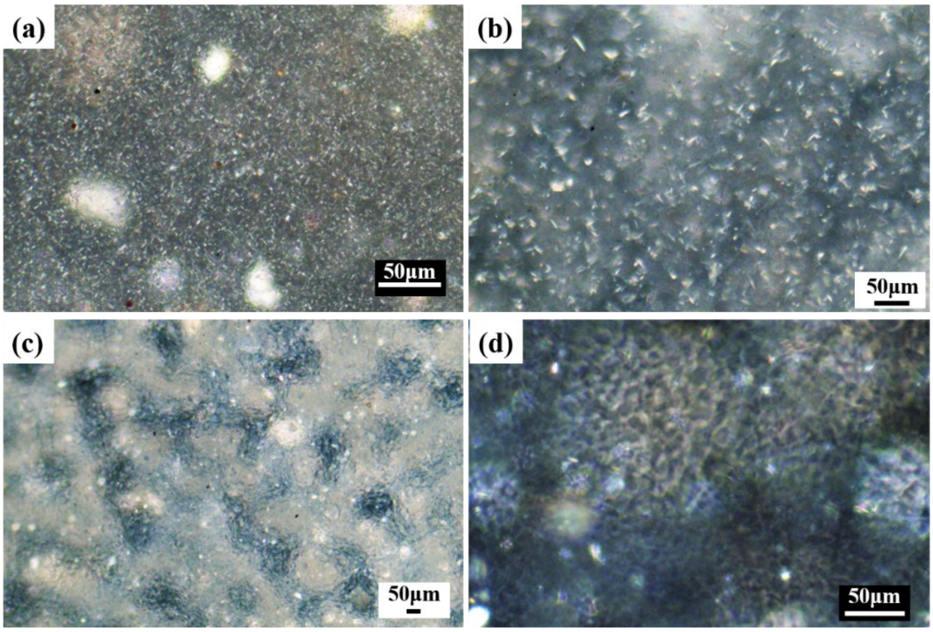

Figure S4. POM images of SIGs at 2% (w/v), (a) NG6-IL2, (b) NG12-IL2, (c) NG18-IL2 and (f)

NGO18-IL2.

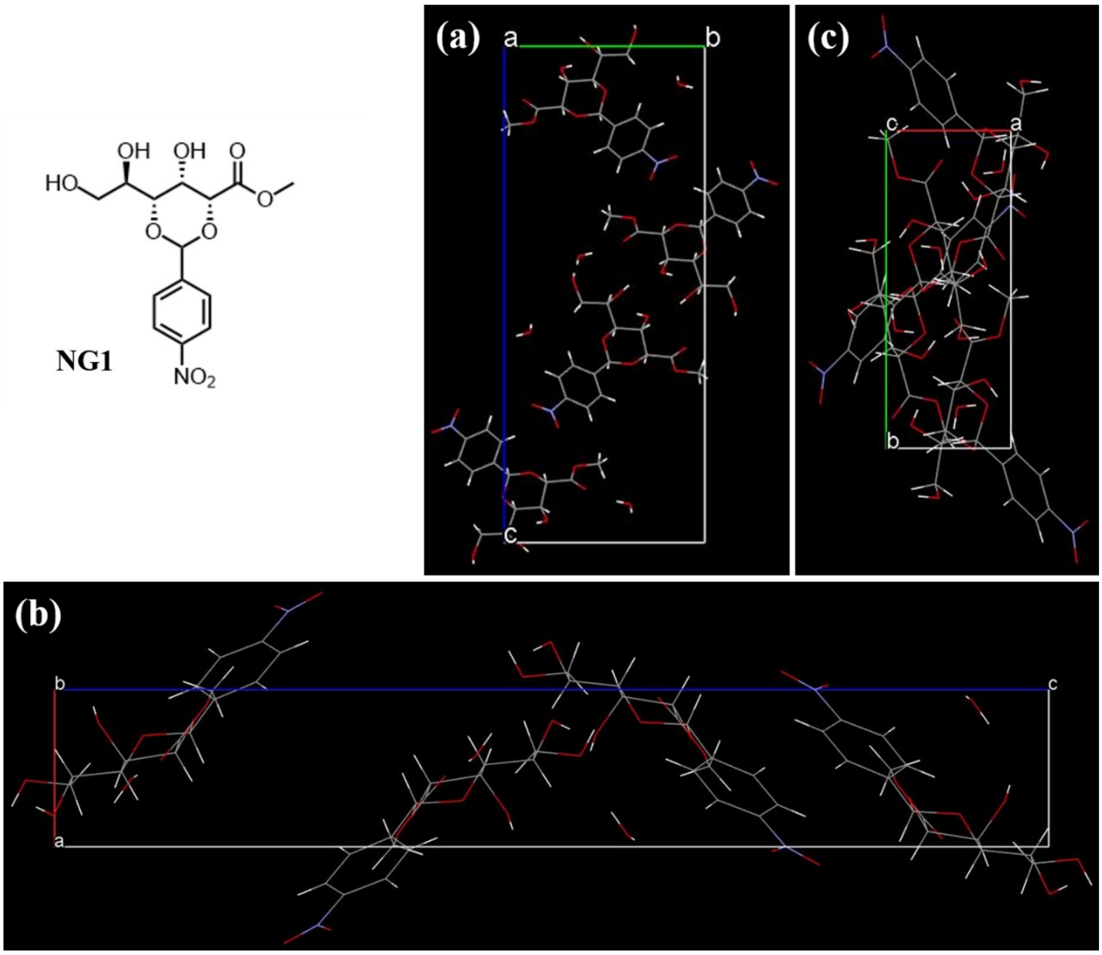

Figure S5. The chemical formula of NG1 and unit cell of the co-crystal of NG1 and H_2O along the (a) a-axis, (b) b-axis, (c) c-axis. Color code: C = gray; H = white; O = red.

Table S2. Crystallographic details of the co-crystal of NG1 and H_2O.

CCDC No.	2130036
Formula	$C_{14}H_{19}NO_{10}$
Formula weight	361.30
Crystal system	Orthorhombic
Space group	$P2_12_12_1$
T, K	149.99
λ (Cu Kα), Å	1.54184
a, Å	4.61033(12)
b, Å	11.7809(4)
c, Å	29.1594(12)
α, °	90

β, °	90
λ, °	90
V, $Å^3$	1583.76(9)
Z	4
Dx, g cm^{-3}	1.515
μ, mm^{-1}	1.133
F (000)	760.0
GOF	1.105
R1	0.0515
wR2	0.1056

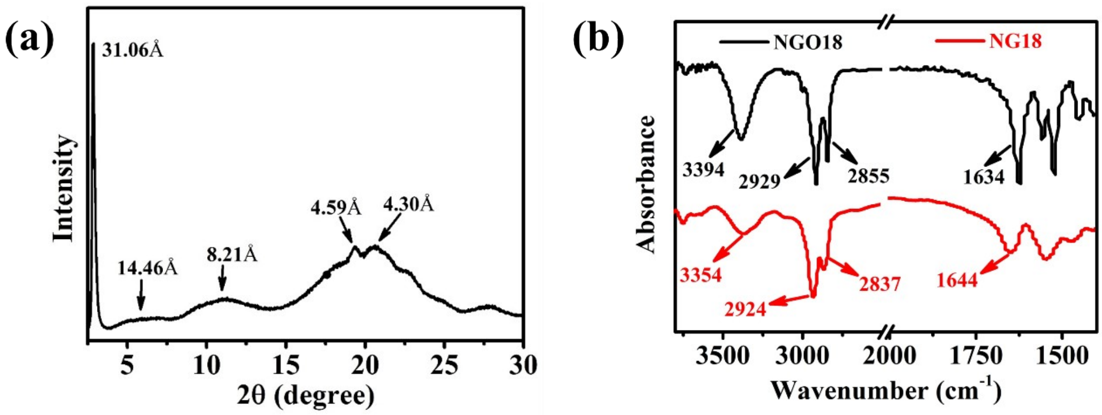

Figure S6. (a) XRD spectra of NGO18 xerogel, (b) FT-IR spectra of NGO18 and NG18 xerogel.

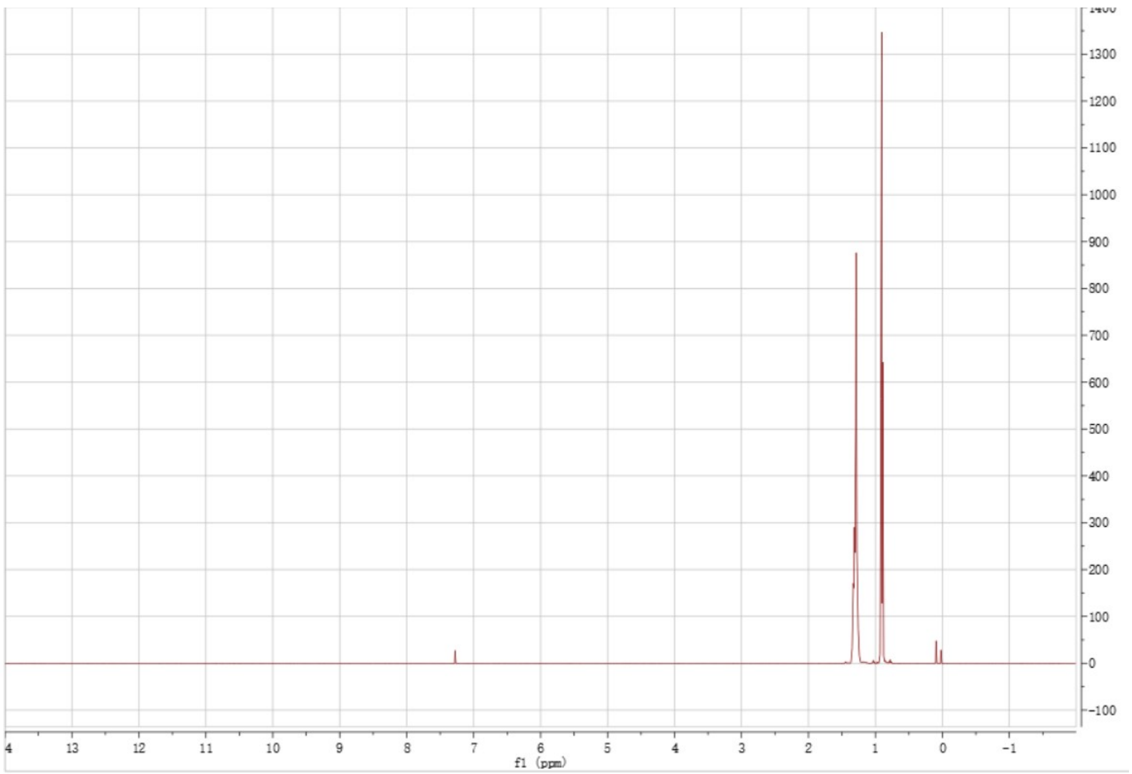

Figure S7. ^{1}H-NMR spectra of hexane which were contacted with NG18-IL2 SIG for 48h.

All the ^{1}H-NMR spectra of hexane contacted with other SIGs were as same as **Figure S6**.

Table S3. The EE value of pure ILs and different SIGs for single sulphur compound.

Gelator/IL		IL1			IL2			IL3			IL4		
	Sulphur Compound	12h	24h	48h	12h	24h	48h	12h	24h	48h	12h	24h	48h
		EE values (%)			EE values (%)			EE values (%)			EE values (%)		
Without Gelator	T	33.9	38.0	37.6	67.2	76.6	76.4	63.5	75.2	75.8	73.6	76.1	76.1
	BT	43.3	44.2	44.0	47.9	56.3	56.0	36.1	50.2	50.0	50.5	62.0	62.0
	DBT	41.0	42.2	42.1	41.0	54.6	54.4	38.9	60.0	59.8	16.1	54.8	54.8
NG6	T	✝			83.3	82.0	81.6	77.1	89.6	90.0	63.5	77.6	77.5
	BT				44.8	74.9	75.0	34.8	82.5	82.5	51.0	62.2	62.3
	DBT				36.4	57.2	57.0	36.7	77.5	77.2	43.8	48.2	48.2
NG12	T	✝			83.6	80	80.2	75.8	97.7	97.6	80.1	81.3	81.0
	BT				40.7	53.1	53.0	16.0	62.4	62.4	35.6	61.2	60.5
	DBT				36.2	52.6	52.8	32.6	49.3	49.6	26.8	56.5	56.1
NG18	T	35.2	39.3	39.1	75.4	76.4	76.3	75.7	78.0	78.1	80.1	78.0	78.6
	BT	42.1	46.5	45.2	57.3	56.0	56.5	54.1	63.2	63.0	60.1	63.9	63.2

	DBT	40.0	43.4	43.4	54.7	52.4	52.3	54.9	60.4	60.0	51.7	56.4	56.0
NGO18	T	24.7	31.6	30.4	52.7	79.4	77.4	72.8	76.0	76.7	70.3	77.0	76.5
	BT	39.5	41.1	41.0	49.1	52.9	50.7	52.0	60.3	56.4	50.8	59.5	57.2
	DBT	39.1	40.1	40.1	33.8	44.9	40.5	54.0	53.1	53.3	51.1	54.5	51.9

Table S4. EE values of NG18-IL2 SIG for T, BT and DBT in desulphurization for solution of mixed sulphur compounds.

SIG/Sulphur compounds	T	BT	DBT
	EE values (%)		
NG18-IL2	40.99	49.76	51.68

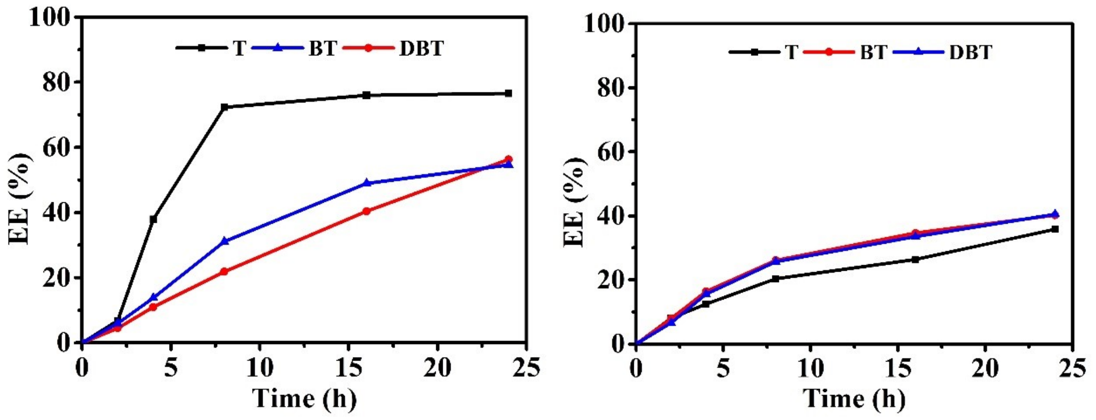

(a) **(b)**

Figure S8.[a] EEs of IL2 for T, BT, and DBT in **(a)** solutions of single sulphur compound and **(b)** solution containing mixture of sulphur compounds as a function of extraction time.

[a] For IL2, during the extraction of sulphur compounds present individually (**Figure S8a**), T was also rapidly cleared in the first four hours and the EE value of T reached its maximum at 8 h, and BT and DBT were also slowly cleared during the entire extraction process. In the extraction of the mixture of sulphur compounds (**Figure S8b**), all the sulphur-containing compounds (T, BT and DBT) were also cleared rapidly in the first two hours and then slowly until the EE values reached maximum at 24 h. The adsorption of BT in the desulphurization process of the mixture of sulphur

compounds was also similar to that of the desulphurization process of individual sulphur compounds. The rate of extraction of DBT was also more rapid than that of the desulphurization of individual sulphur compounds. The extraction rate of T was also still rapid in the first two hours of desulphurization of sulphur compound-containing mixture, but its maximum EE value also deceased, as compared to the desulphurization of individual sulphur compounds.

Table S5. EE values of NG18-IL2 SIG for T, BT and DBT in extraction tests at different concentrations.

Concentrations of model fuel/ Sulphur compounds	T	BT	DBT
	EE values (%)/ Adsorptive quantity (mg)		
1000 ppm	41.75/0.14	55.06/0.18	55.17/0.18
1500 ppm	40.99/0.21	49.76/0.25	51.68/0.26
2000 ppm	37.89/0.25	42.09/0.28	43.87/0.29
3000 ppm	32.24/0.32	37.57/0.38	38.91/0.39
5000 ppm	20.99/0.35	23.63/0.39	23.39/0.39

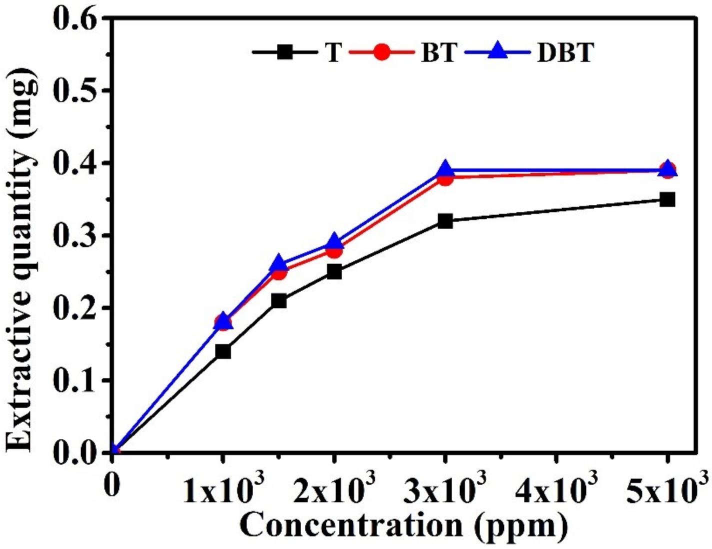

Figure S9. The extractive quantity of NG18-IL2 SIG for T, BT and DBT in extraction tests at different concentrations.

Table S6. EE values of NG18-IL2 SIG for T, BT and DBT in extraction tests at different fuel volumes.

Volume of model fuel/ Sulphur compounds	T	BT	DBT
	EE values (%)/ Adsorptive quantity (mg)		
400 μl	47.59/0.19	51.09/0.20	52.07/0.21
500 μl	40.99/0.21	49.76/0.25	51.68/0.26
700 μl	37.78/0.26	41.90/0.29	42.84/0.30
1000 μl	29.55/0.30	35.98/0.36	37.98/0.38
1500 μl	23.34/0.35	23.32/0.37	21.33/0.38

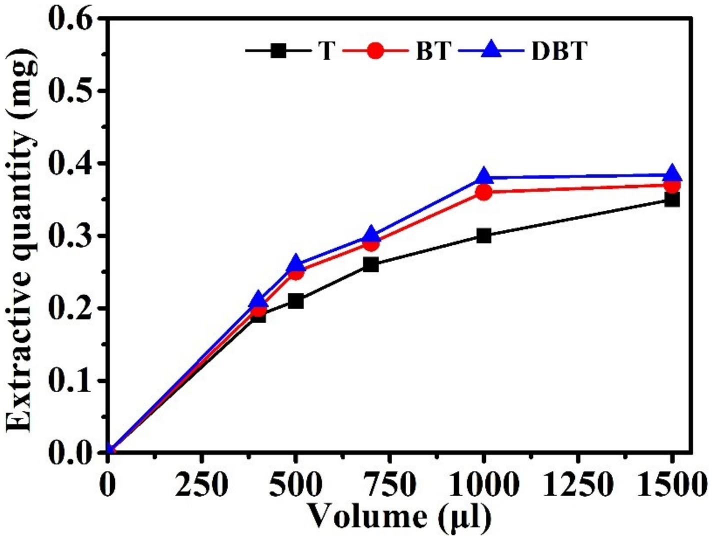

Figure S10. The extractive quantity of NG18-IL2 SIG for T, BT and DBT in extraction tests at different fuel volumes.

Table S7. EE values of NG18-IL2 SIG for T, BT and DBT in extraction tests at various temperature.

Temperature/ Sulphur compounds	T	BT	DBT
	EE values (%)		
25°C	40.99	49.76	51.68
30°C	32.95	39.96	40.67
40°C	29.42	29.36	29.98
50°C	22.57	18.14	18.75

Table S8. EE values of NG18-IL2 SIG for T, BT and DBT in every extraction stage.

Number of extraction stage/ Sulphur compounds	T	BT	DBT
	EE values (%)		
1	40.99	49.76	51.68
2	90.02	89.85	80.93
3	100	98.87	98.02
4	100	100	100

Table S9. EE values of NG18-IL2 SIG for T, BT and DBT in every reuse cycle.

Cycles/ Sulphur compounds	T	BT	DBT
	EE values (%)		
1	40.99	49.76	51.68
2	35.15	32.26	36.30
3	26.39	16.44	18.17
4	25.78	19.78	19.92
5	23.70	15.23	16.54
6	20.18	6.07	8.73
7	19.58	0	0

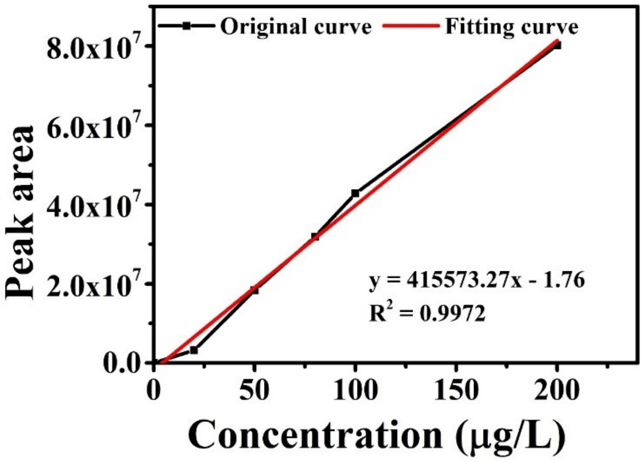

Figure S11. Mass spectrum peak area values of standard IL2 solutions with different concentration detected by LMS (shown as **black line**). The mass peak areas of 20μg/L, 50μg/L, 80μg/L, 100μg/L, and 200μg/L IL2 methanol solutions are 3226231, 18350415, 31854692, 42822660, and 80194082, respectively. The fitted curve is shown as the **red line**, and the corresponding fitting equation is also given. The mass spectrum peak area of 1-butyl-1-methylpyrrolidine cation in 2ppb methanol solution of sample was detected as 24932305, and the concentration of IL2 could be calculated as 178μg/L.

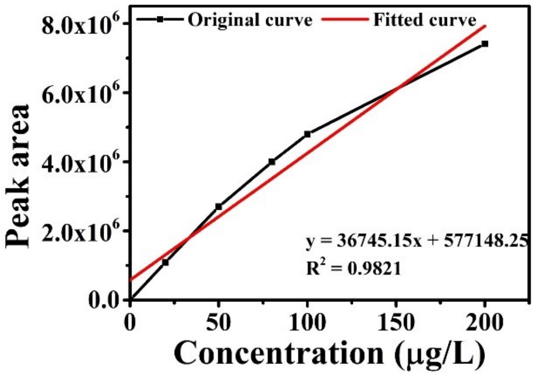

Figure S12. Mass spectrum peak area values of standard NG18 solutions with different concentration detected by LMS (shown as **black line**). The mass peak areas of 20μg/L, 50μg/L, 80μg/L, 100μg/L, and 200μg/L NG18 methanol solutions are 1088625, 2700137, 3998719, 4801181, and 7409547, respectively. The fitted curve is shown as the **red line**, and the corresponding fitting equation is also given. The mass spectrum peak area of NG18 in 2ppb methanol solution of sample was detected as 705756.28, and the concentration of NG18 could be calculated as 3.5μg/L.

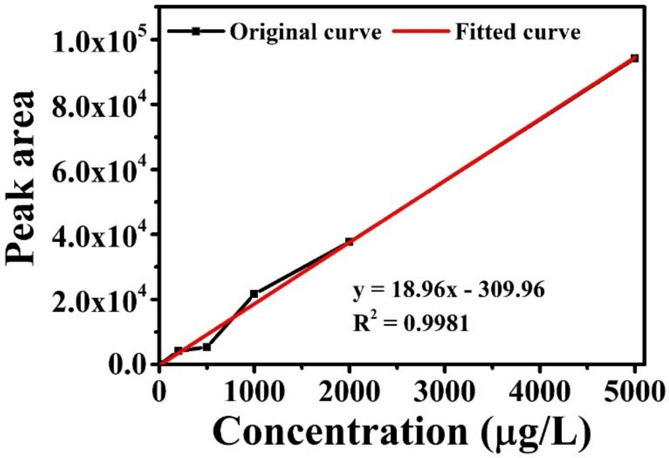

Figure S13. Mass spectrum peak area values of standard BT solutions with different concentration detected by LMS (shown as **black line**). The mass peak areas of 500 μg/L, 200 μg/L, 100 μg/L, 50 μg/L, and 20 μg/L BT methanol solutions are 9479, 3791, 2168, 947, and 379, respectively. The fitted curve is shown as the **red line**, and the corresponding fitting equation is also given. The mass spectrum peak area of BT in 2ppb methanol solution of sample was detected as 40.8, and the concentration of BT could be calculated as 18.5μg/L.

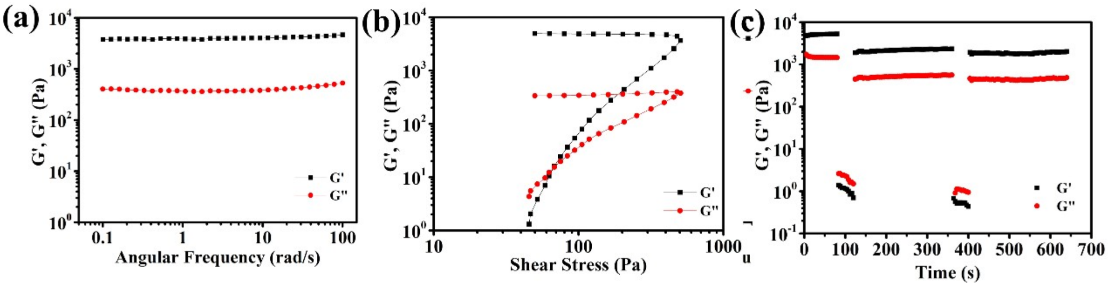

Figure S14. Oscillatory rheological study of regenerated SIG. (a) Frequency sweep, (b) strain sweep and (c) step-strain measurement. The detailed rheological data were summarized in **Table S13** below.

Table S10. Rheological data of regenerated SIG (2% w/v)

G’ (Pa)[a]	**G1’ (Pa)[b]**	**G2’ (Pa)[c]**	**η (%)**	**tanδ**	**Strain stress at flow point (Pa)**
4750	2343	2043	49.3	0.24	66.78

Table S11. EE values of NG18-IL2 SIG with different regeneration times for T, BT and DBT.

Number of regenerations / Sulphur compounds	T	BT	DBT
	AE values (%)		
1	39.30	38.50	43.36
2	32.50	35.36	36.20
3	33.60	32.40	35.70
4	33.00	34.10	35.90

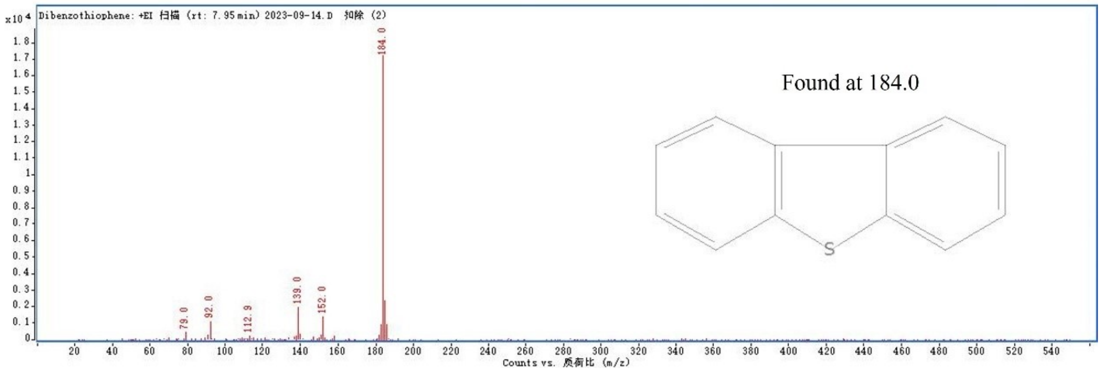

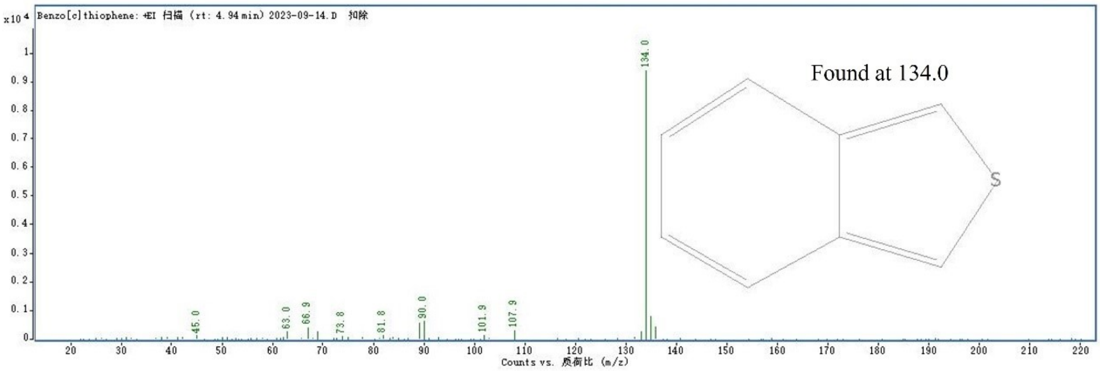

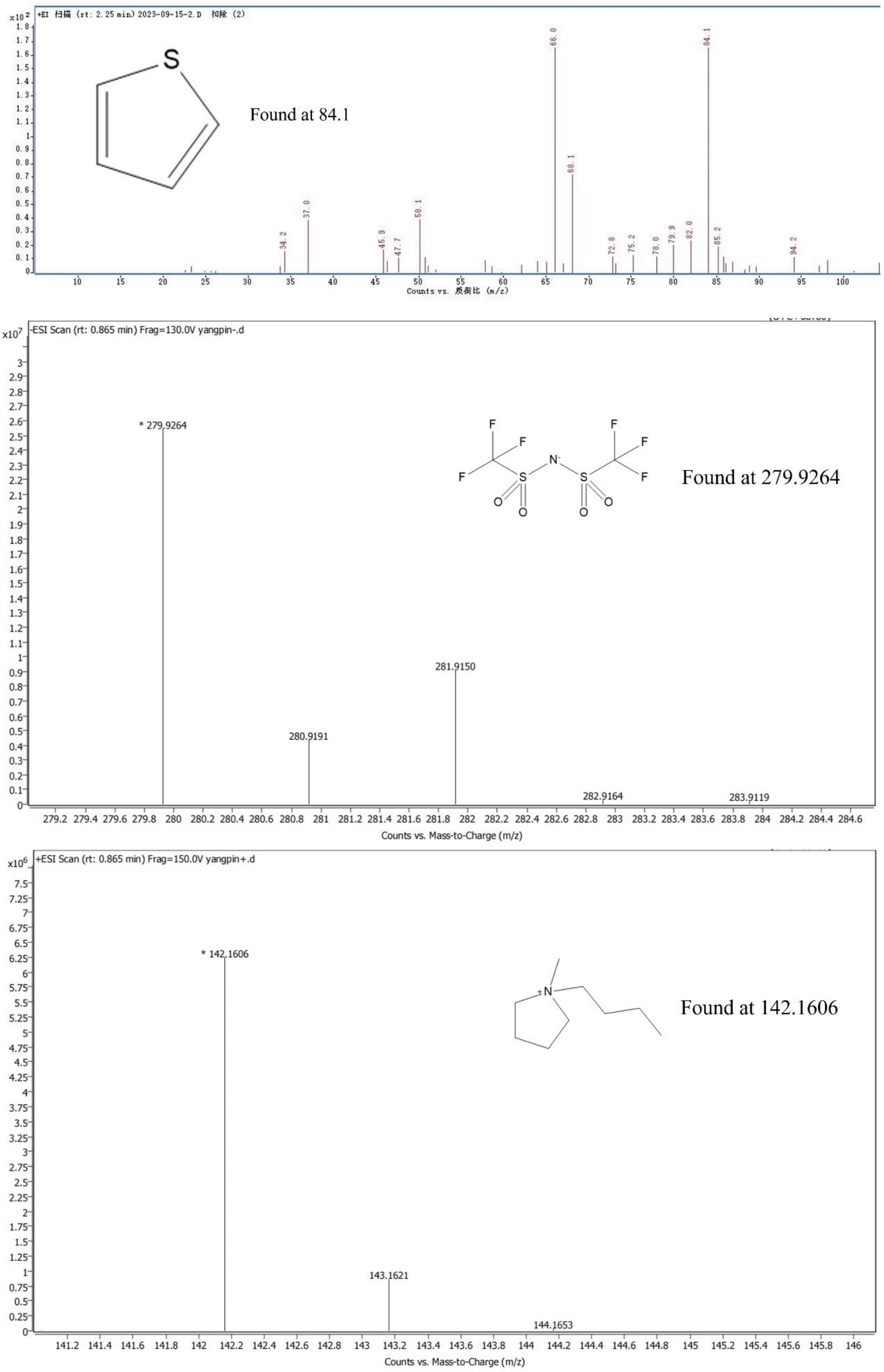

Figure S15. Mass spectrum of T, BT, DBT, and anion and cation of IL2 provided by LCMS or

GCMS.

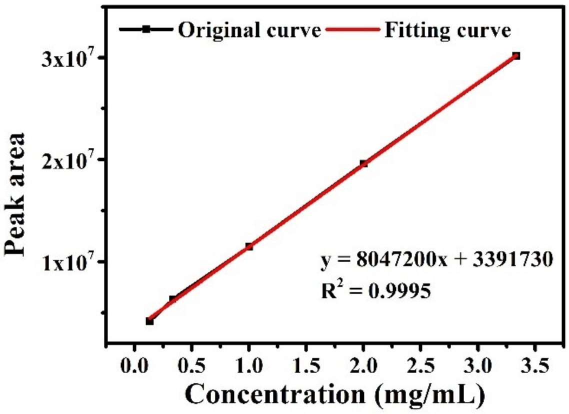

Figure S16. Mass spectrum peak area values of standard T solutions with different concentration detected by GCMS (shown as **black line**). The mass peak areas of 0.1334 mg/mL, 0.3335 mg/mL, 1.0005 mg/mL, 2.001 mg/mL, and 3.335 mg/mL T methanol solutions are 4167051.86, 6324789.51, 11469347.61, 19602669.48, and 30143147.98, respectively. The fitted curve is shown as the **red line**, and the corresponding fitting equation is also given. The mass spectrum peak area of T in aqueous phase was detected as 5001170.12, and the concentration of T could be calculated as 0.2 mg/mL.

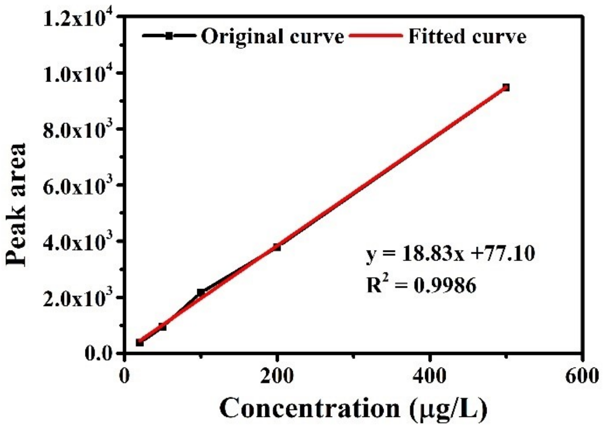

Figure S17. Mass spectrum peak area values of standard BT solutions with different concentration detected by LMS (shown as **black line**). The mass peak areas of 20 μg/L, 50 μg/L, 100 μg/L, 200 μg/L, and 500 μg/L BT methanol solutions are 379, 947, 2168, 3791, and 9479, respectively. The fitted curve is shown as the **red line**, and the corresponding fitting equation is also given. The mass spectrum peak area of BT in aqueous phase was detected as 2786917.10, and the concentration of BT could be calculated as 148mg/L.

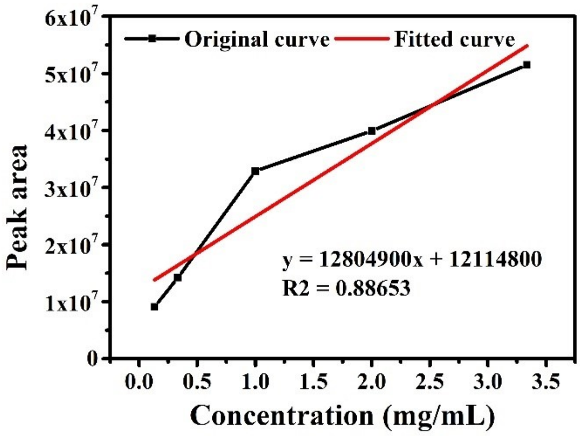

Figure S18. Mass spectrum peak area values of standard DBT solutions with different concentration detected by GCMS (shown as **black line**). The mass peak areas of 0.1334 mg/mL, 0.3335 mg/mL, 1.0005 mg/mL, 2.001 mg/mL, and 3.335 mg/mL DBT methanol solutions are 9089245.07, 14238200.93, 32914448.81, 39949231.77, and 51499387.3, respectively. The fitted curve is shown as the **red line**, and the corresponding fitting equation is also given. The mass spectrum peak area of DBT in aqueous phase was detected as 18773348, and the concentration of BT could be calculated as 0.52mg/mL.

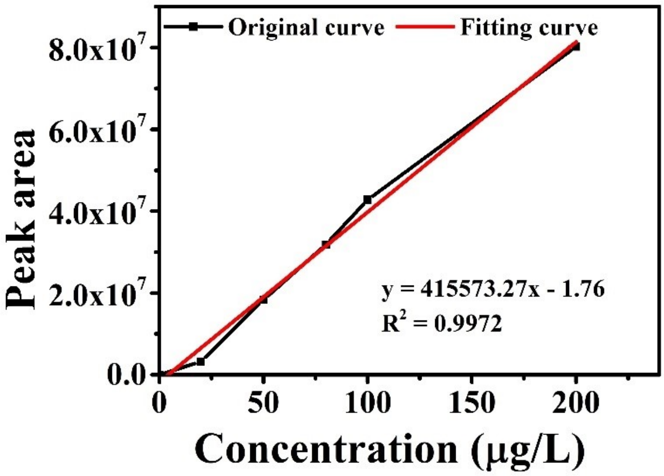

Figure S19. Mass spectrum peak area values of standard IL2 solutions with different concentration detected by LCMS (shown as **black line**). The mass peak areas of 20μg/L, 50μg/L, 80μg/L, 100μg/L, and 200μg/L IL2 methanol solutions are 3226231, 18350415, 31854692, 42822660, and 80194082, respectively. The fitted curve is shown as the **red line**, and the corresponding fitting equation is also given. The mass spectrum peak area of IL2 in aqueous phase was detected as 55936160.38, and the concentration of BT could be calculated as 134.6mg/mL.

Table S12. Oxidation efficiency of T, BT, and DBT by H_2O_2 in aqueous phase at different conditions

$n(H_2O_2)/n(T+BT+DBT)$	Temp. & time	Oxidation efficiency		
		T	BT	DBT
6:1	25°C, 30min	45.09%	25.34%	46.21%
6:1	40°C[a], 30min	51.17%	27.80%	49.57%
6:1	40°C, 60min	69.2%	32.89%	62.28%
12:1	40°C, 60min	51.74%	50.03%	73.77%
18:1	40°C, 60min	65.11%	66.00%	97.01%
20:1	40°C, 60min	75.35%	82.50%	100%
24:1	40°C, 60min	74.96%	83.00%	100%

[a] In order to not only speed up the oxidation rate, but also not to make the reaction too violent to produce by-products, 40°C was employed.

Table S13.[a] The concentration of T, BT, and DBT in the aqueous phase before and after oxidation

	Volume of	Concentration

	aqueous phase	IL2	T	BT	DBT
Before oxidation	40 mL	134.6 mg/mL	0.2 mg/mL	0.148 mg/mL	0.52 mg/mL
After oxidation	90 mL		2.67 μg/mL	6.22 μg/mL	0 μg/mL

[a] The amount of IL2 in the aqueous phase was 134.6mg/mL × 40 mL = 5.38g. After oxidation, the amount of T remaining in the aqueous phase was 2.67 μg/mL× 90 mL = 0.24 mg, and the amount of BT was 6.22 μg/mL× 90 mL = 0.56 mg. After vacuum distillation, extraction, separation and a second vacuum distillation, the final amount of IL2 was 4.621g, which contained 0.24 mg T and 0.56 mg BT. The final recovery rate of IL2 was 4.6202/5.38 = 86%.

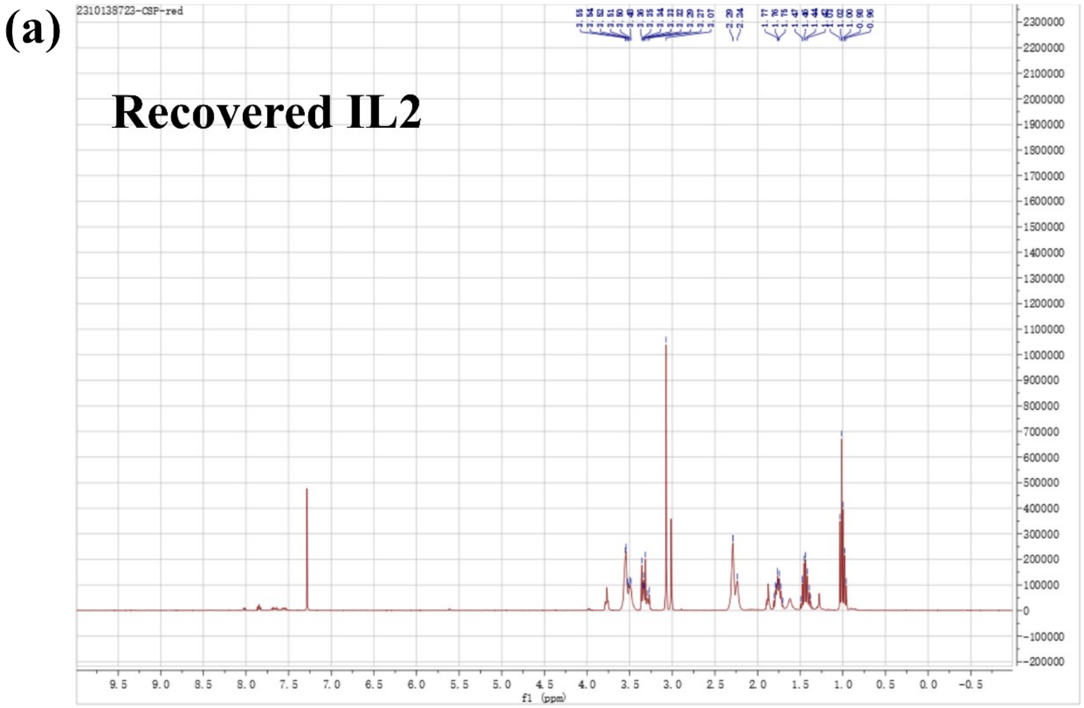

(b)

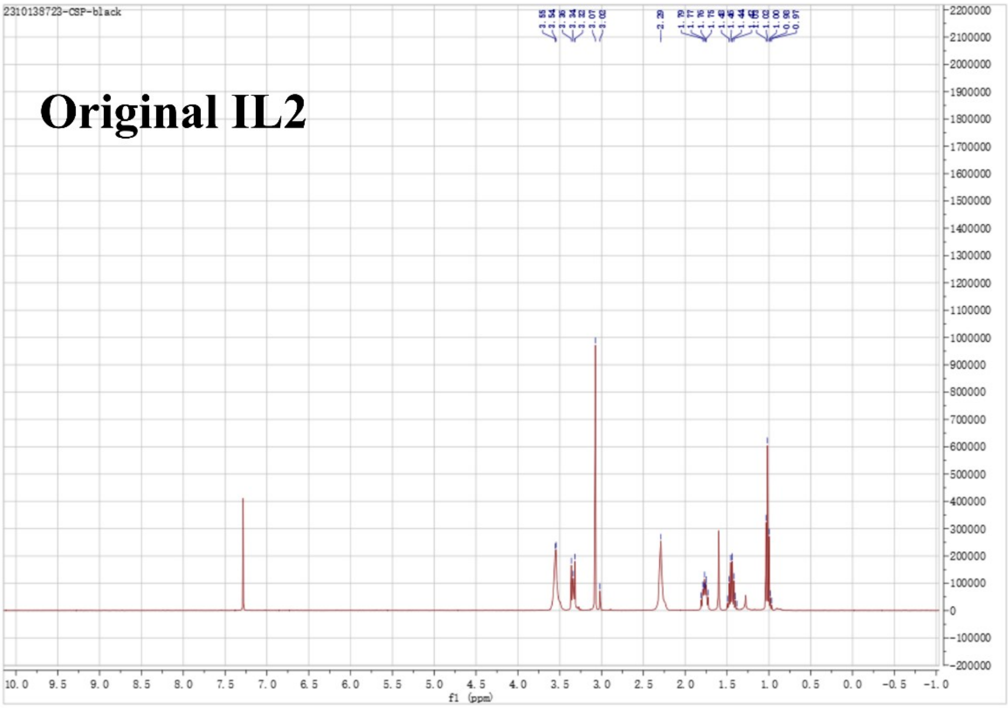
2310138723-CSP-black
Original IL2
3.55
3.54
3.36
3.34
3.32
3.07
3.02
2.29
1.79
1.77
1.76
1.75
1.48
1.45
1.44
1.43
1.02
1.00
0.98
0.97
2200000
2100000
2000000
1900000
1800000
1700000
1600000
1500000
1400000
1300000
1200000
1100000
1000000
900000
800000
700000
600000
500000
400000
300000
200000
100000
0
-100000
-200000
10.0 9.5 9.0 8.5 8.0 7.5 7.0 6.5 6.0 5.5 5.0 4.5 4.0 3.5 3.0 2.5 2.0 1.5 1.0 0.5 0.0 -0.5 -1.0
f1 (ppm)

(c)

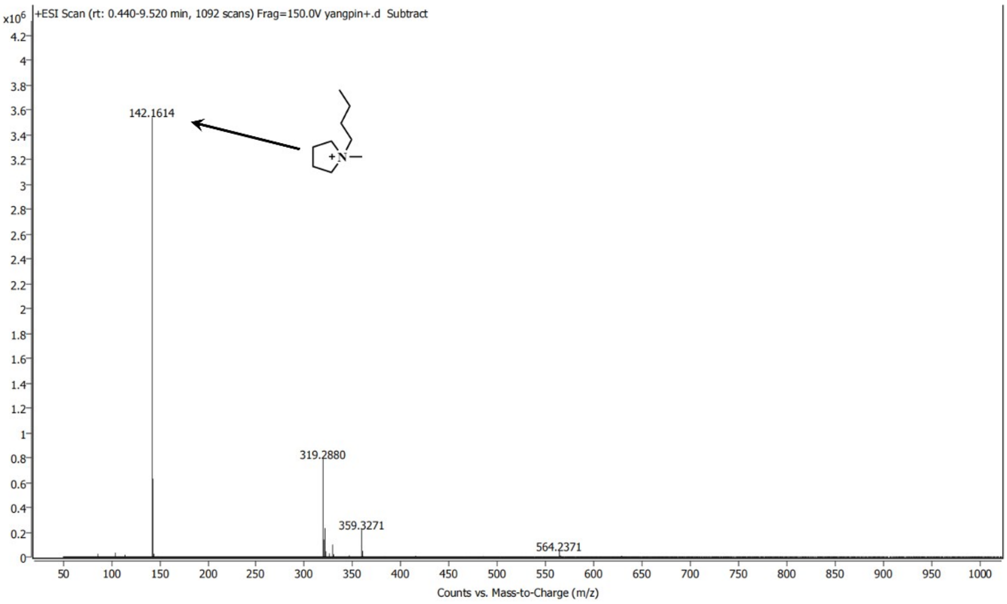
+ESI Scan (rt: 0.440-9.520 min, 1092 scans) Frag=150.0V yangpin+.d Subtract
x10^6
4.2
4
3.8
3.6
3.4
3.2
3
2.8
2.6
2.4
2.2
2
1.8
1.6
1.4
1.2
1
0.8
0.6
0.4
0.2
0
142.1614
+N
319.2880
359.3271
564.2371
50 100 150 200 250 300 350 400 450 500 550 600 650 700 750 800 850 900 950 1000
Counts vs. Mass-to-Charge (m/z)

(d)

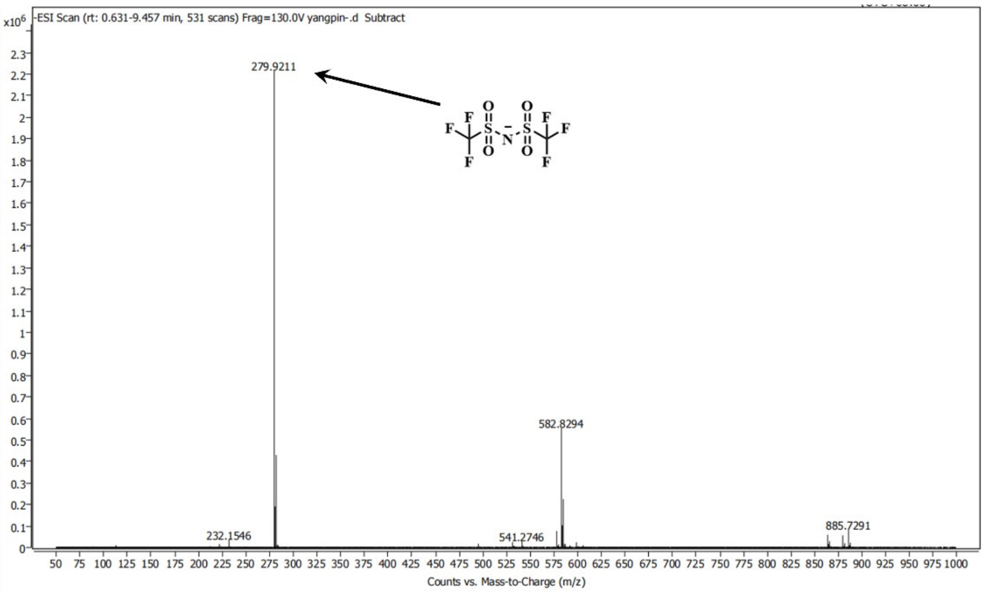

Figure S20. ^{1}H-NMR ($CDCl_3$) spectrum of **(a)** recovered IL2 and **(b)** original IL2, and Mass spectrum of **(c)** cation and **(d)** anion of recovered IL2. As shown in **Figure S17a**, ^{1}H-NMR characteristic peaks of original IL2 were δ 3.55 (d, 4H), 3.34 (m, 2H), 3.07 (s, 3H), 2.29 (s, 4H), 1.77 (M, 2H), 1.44 (m, 2H), 1.0 (m, 3H). All these peaks could be found in ^{1}H-NMR spectrum of recovered IL2. In addition, the mass peak of cation ($C_4C_1pyr^+$) and anion ($TFSA^-$) could be found in mass spectrum of recovered IL2. Therefore, the chemical structure of the recovered IL2 was consistent with that of the original IL2.

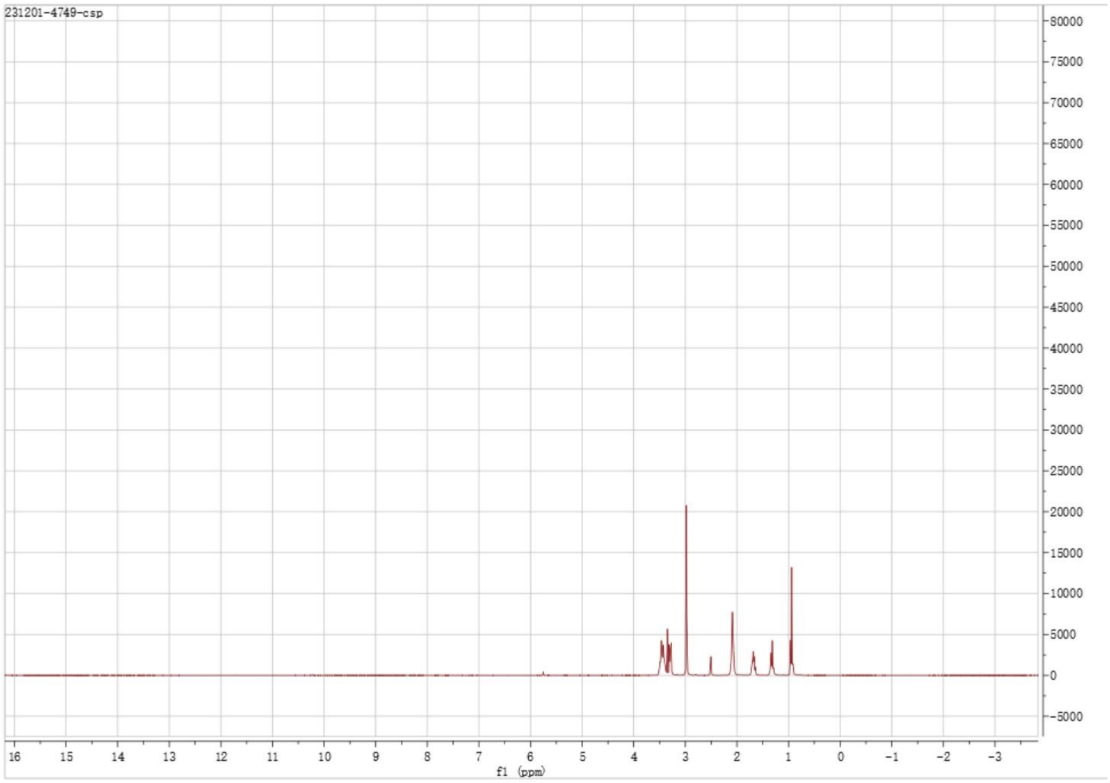

Figure S21. ^{1}H-NMR (d_6-DMSO) spectrum of recovered IL2 extracted with hexane. The spectra is identical with that of the original IL2 (**Figure S20b**).

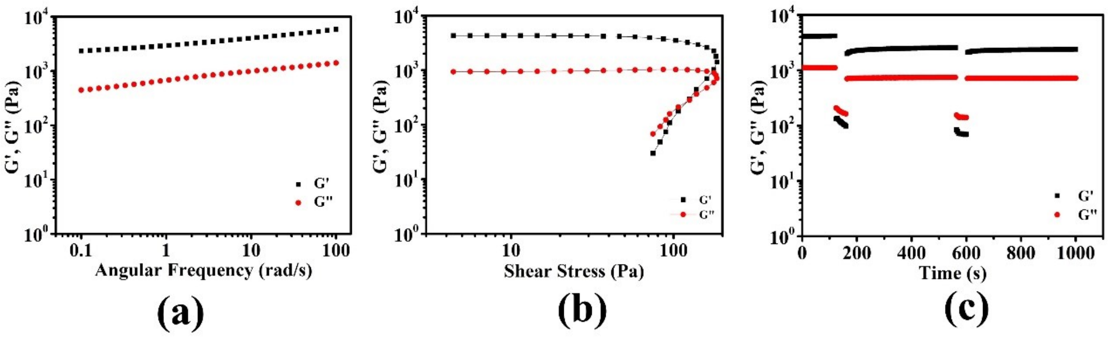

Figure S22. Oscillatory rheological study of SIGs prepared by IL2 recovered from aqueous phase produced in the process of NG18-IL2 SIG regeneration. (a) Frequency sweep, (b) strain sweep and (c) step-strain measurement. The detailed rheological data were summarized in **Table S13** below.

Table S14. Rheological data of SIG (2% w/v) prepared by IL2 recovered from aqueous phase

G’ (Pa)[a]	**G1’ (Pa)**[b]	**G2’ (Pa)**[c]	**η (%)**	**tanδ**	**Strain stress at flow point (Pa)**
4295	2566.5	2388.3	62.5	0.19	120.9

produced in the process of NG18-IL2 SIG regeneration